SINTECHCOM: Science, Technology and Communication Journal
Vol. 2, No. 2, February 2022, pp. 55-62, DOI: 10.59190/stc.v2i2.208

A numerical study on T-reduce junction flow distribution

Haryadi*, Sugianto, Ali Mahmudi, Radi Suradi Kartanegara
Department of Mechanical Engineering, Politeknik Negeri Bandung, West Bandung 40559, Indonesia

ABSTRACT

Although many manifold shapes have been studied, research on venturi-shaped manifolds with holes smaller than the inner diameter of the pipe, hereinafter referred to as T-reducer, has so far not been found. This research studies the effect of hole diameter and Reynolds number on the debit that comes out of the branch pipe. The venturi hole diameter is varied from 40% to 80% of the main pipe diameter, while the bulk velocity is varied from 2 to 10 m/s. The research started by creating a 3D T-reducer model, followed by CFD simulation using Fluent software. From the simulation results, curve fitting is performed using multiple regression to obtain an equation which is the correlation of dimensionless numbers. The maximum difference between the flow coefficient obtained from the curve fitting equation and the CFD simulation results is 3.35%.

ARTICLE INFO

Article history:

Received Jan 2, 2022
Revised Jan 20, 2022
Accepted Feb 25, 2022

Keywords:

CFD
Correlation Equation
Junction
T-Reducer
Venturi

* **Corresponding Author**
E-mail address: haryadi.mesin@polban.ac.id

1. INTRODUCTION

Different types of flow dividers and manifolds are used in industries, such as power plants, process industries, water treatment plants, etc. Manifolds can be divided into dividers and combiners (unifiers) [1, 2]. The flow dividing manifold is used to divide a flow into several streams with a smaller debit, while the combining manifold is used to combine or unite several small streams into one stream with a larger flowrate [3-5].

Figure 1 shows some of the shapes and directions of flow in a pipe. In terms of the number of output streams, the split manifold can be divided into manifolds with two outlets, and a manifold with three or more outlets. And also the combining manifold can be divided into manifolds with two inlets, three or more outlets. In terms of the direction of the outlet flow, the manifold can also be divided into three, namely direct flow (parallel), perpendicular flow, and reverse flow. In a unidirectional manifold, the outflow is in the direction of the inflow, the outflow is perpendicular to the inflow, and in reverse flow, the outflow is opposite to the inflow. In terms of shape, manifolds can be divided into two, namely Y (or fork) and T forms. In terms of laying, manifolds can generally be divided into 2, namely horizontal and vertical.

Distribution manifolds are usually used to obtain an even flow distribution, such as in heat exchangers [6, 7]. In general, the manifold has the same diameter between the main pipe (header) and the branch pipe. It's just that for the need for greater discharge reduction, the manifold neck can be reduced [8-10]. In this work, a numerical study of a dividing venturi-shaped manifold with holes smaller than the inner diameter of the pipe, hereinafter referred to as T-reducers, with 2 T-shaped outlets with a perpendicular output direction will be presented. The manifold is in horizontal placement, with a neck diameter smaller than the diameter of the main pipe, as shown in Figure 2. To improve flow properties and avoid cavitation, the diameter of the neck will be gradually increased to produce a conical neck shape. The neck diameter is varied from 30% to 80%.

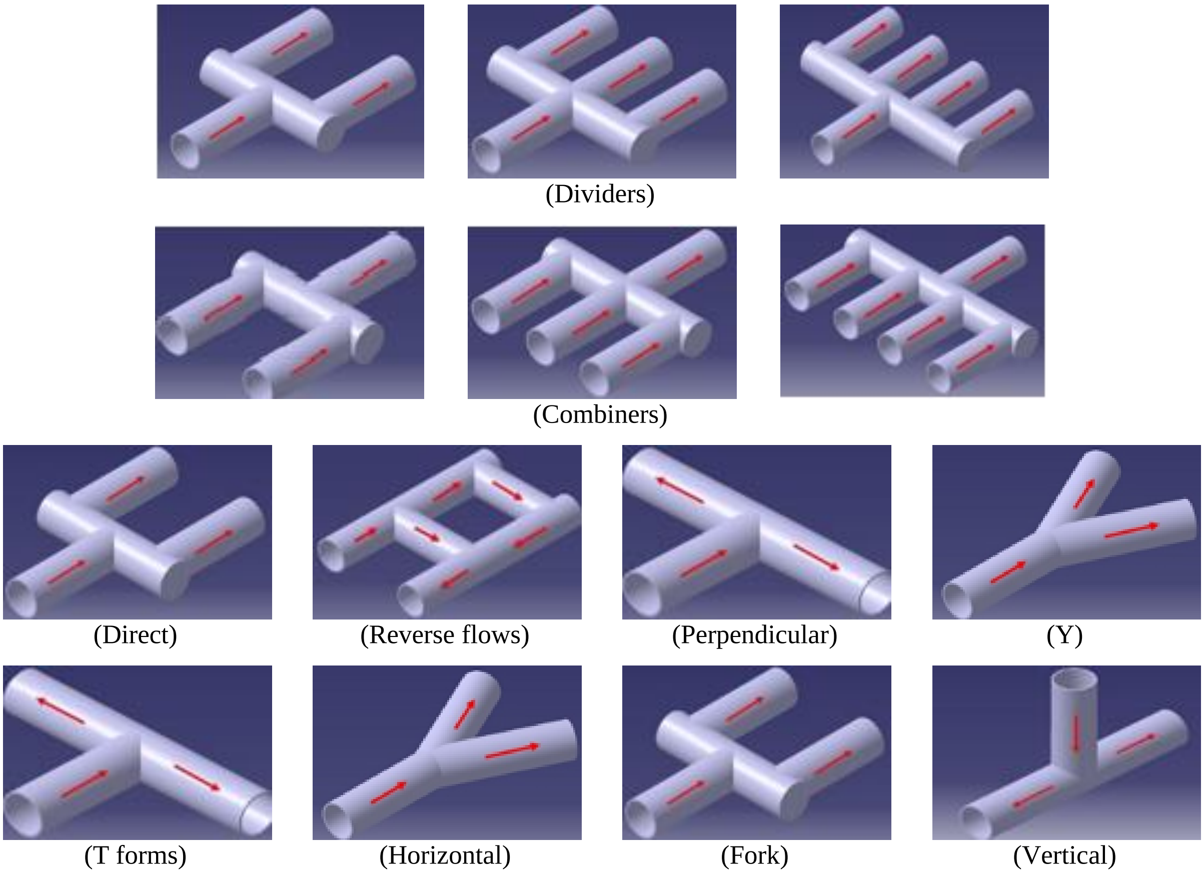

Figure 1. Types of manifold.

Manifold flow has been studied by many researchers. Hassan et al. (2014) have researched on a splitting manifold with 5 T-shaped outputs, with horizontal placement, uniform diameter. The study was carried out numerically and experimentally. The results of the study show that there is a maldistribution of the five output pipes. The flow distribution value at Re 150,000, for the first outlet pipe to the 5th pipe respectively, are 14%, 17%, 20%, 20%, 24%, and 25%. The research was also carried out on Re 100,000 and 200,000. In both Re numbers, the flow distribution does not change much. In addition, it is also concluded that the simulation results with CFD are quite close to the experimental results. Furthermore, the research was continued by using a cone manifold. This manifold provides a more even distribution [11].

Phase maldistribution has negative and positive consequences for the equipment used. The negative side of the occurrence of phase maldistribution will cause a decrease in the efficiency of the equipment used in the downstream section of the T-junction [12] and the positive side of the phase maldistribution that occurs in the T-junction can be used as a useful tool in industrial processes, namely phase separation. The phase separation process using a T-junction was first introduced by Oranje in 1973 which investigated the separation of the flow of two liquid gas phases [13] and the T-junction as a partial phase separator [14].

A lot of research on T-Junction has been done. Sugianto et al. (2010), studied the use of T-Junction for water-kerosene separation, focusing on the effect of branch pipe diameter. The study was conducted using CFD and validated by experiment. Kerosene tends to flow into the branch pipe that leads vertically. The larger the diameter of the branch pipe, it tends to produce a larger kerosene fraction [15]. Tran et al. (2018) also investigated the separation of the two-phase water-air flow at the T-Junction, in the slug-flow regime. Numerical modeling shows that the reduced T-junction gives better results than the regular T-junction [16]. Wu et al. (2019) investigated the characteristics of the two-phase separation of viscous oil from water in the T manifold with multiple outputs. The results of this study indicate that the number of outputs and the distance between the outputs (spacing) have a major effect on the efficiency of separation. A larger number of outputs tends to increase the efficiency of the separation. The output height has no significant effect on efficiency. Meanwhile, the wider the spacing, the efficiency of the separation increases, and tends to lose its effect at 7D spacings or more [17]. Yang et al. (2019) investigated the double layer T-junction for the separation of water and oil. Research shows that the effect of oil fraction is less significant than the inlet velocity. The separation efficiency tends to decrease with increasing water velocity [18]. Berman et al. (2018) investigated the effect of using a T-junction flash gas bypass refrigerant on the performance of the AC system. The use of T-junctions can increase the COP and reduce the electric power consumption for the compressor [19].

T-junction problems also occur in the aircraft's hydraulic system. There is a decrease in pressure at the T-junction which can affect the work of the hydraulic system. This research was conducted by Li and Wang (2013) using the shear stress transport (SST) model in ANSYS/CFX software. The investigated T-junction has a curvature at the branch pipe. The curvature radius was varied. The results showed that a certain radius of curvature resulted in the smallest pressure drop [20].

Other studies that utilize the T-junction as a fluid phase separator include the process of separating the two-phase gas-liquid flow in an annular flow pattern [21], the effect of flow patterns on gas-liquid separation [22], the process of analysis and determination of related variables. with fluid flow separation namely gas flow rate, quality in each branch and pressure drops associated with branching [23], separation of liquid-liquid phases namely kerosene and water with a stratified flow pattern [24], and separation of liquid-liquid phases namely kerosene and water with a stratified flow pattern with mixture interface (ST & MI) and a dispersed flow pattern [25].

Research on the two-phase flow pattern in the pipe or in the T-junction has also been carried out by many researchers, including; flow prediction scheme in a horizontal T-junction, a grouping of two-phase liquid-liquid flow patterns into stratified - stratified flow patterns with mixing interface and dispersed, a grouping of two-phase water-oil flow patterns through horizontal pipes into stratified smooth (ST) - stratified wavy (SW) - stratified flow with mixing at the interface [26], as well as visualization studies and two-phase air-water flow patterns in horizontal pipes and branching pipes that have varying angles at the branching points [27].

Many researchers have conducted research on mathematical modeling and/or numerical simulation of two-phase flow in a pipe or T-junction, including numerical simulation of two-phase water-oil flow in a T-junction using the turbulent mixture κ-ε model [28], numerical simulation of the gas-oil two-phase flow pattern in a horizontal pipe using the volume of fluid (VOF) technique [27], numerical simulation of the gas-oil two-phase flow in a narrowed T-junction at the branching angle using the principle of pressure equilibrium , mass, momentum and energy [28], numerical simulation of two-phase water-tetradecane flow drop formation in the T-junction using VOF technique [29], CFD analysis for pressure drop prediction of two-phase refrigerant flow using a two-phase model Fluent [30], modeling the flow of two-phase refrigerant in a short orifice tube [31], as well as a comparison of the commercial computational multi fluid dynamics (CMFD) tracking interface capacity namely VOF method-Fluent and level set method-TransAT [32]. Based on the results of research which conducted a comparative study of the VOF and LS models, it was found that VOF meets mass conservation and is not good for the results of a two-phase tracking interface and vice versa LS does not meet mass conservation and is very good at producing a two-phase tracking interface. From the studies above, it can be concluded that the T-junction can be used to separate two-phase flows, and of course, it can be used as a divider in single-phase flows.

2. MATERIALS AND METHOD

Figure 2 shows an isometric cross-section of the T-reduce junction, which the characteristics will be studied in this study, namely the effect of flow velocity and orifice diameter on the distribution of discharge. Pipes of inner diameter *D* have branches in a perpendicular horizontal direction of the same diameter. Diameter *D*, this remains at 247 mm, obtained from a pipe with a nominal diameter of 10 in, schedule 80. The branch mouth is venturi-shaped with diameter *d*, with a conical section of 1.86 *D* long. This venturi shape is intended to reduce the possibility of cavitation. Water enters with a *Q1* debit, exits towards the front with a *Q2* and to the side with a *Q3*. The venturi neck is given a 5 mm radius.

The flow rate was varied from 0.0927 m^3/s to 0.4635 m^3/s (or at a bulk velocity of 2 m/s to 10 m/s), which corresponded to the Reynolds number, Re between 4.83×10^5 to 2.41×10^6. While the diameter of the neck of the venturi *d*, varied from about 30% to 80%, which became slightly larger due to the increase in the radius of the neck. Both ends of the outlet pipe are not pressurized. The junction is in a horizontal position.

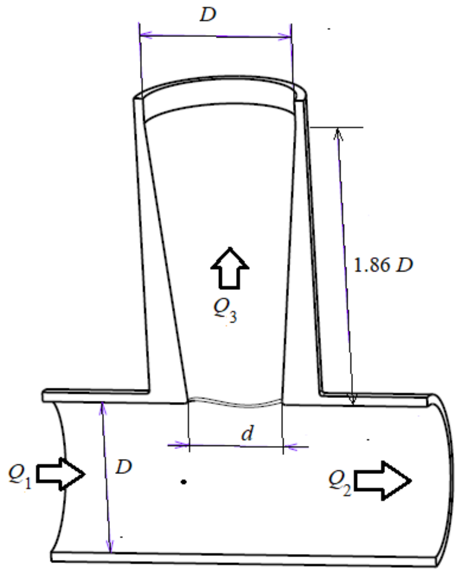

Figure 2. T-reduce junction.

To solve this problem, the CFD software of Fluent was employed. The solver was 3D steady flow, single phase. Cylindrical pipes were added at the inlet and outlet, to ensure that near steady flow condition has been reached. The working fluid was water. The turbulence model was $\kappa - \varepsilon$. The boundaryconditions weredefined velocity at inlet,constant pressure at the two outlets.

Figure 3 shows meshing to the model. The mesh was hexagonal brick for the cylinder part, polygonal around neck of the venturi. A special mesh polygonal form was employed for the transition region.

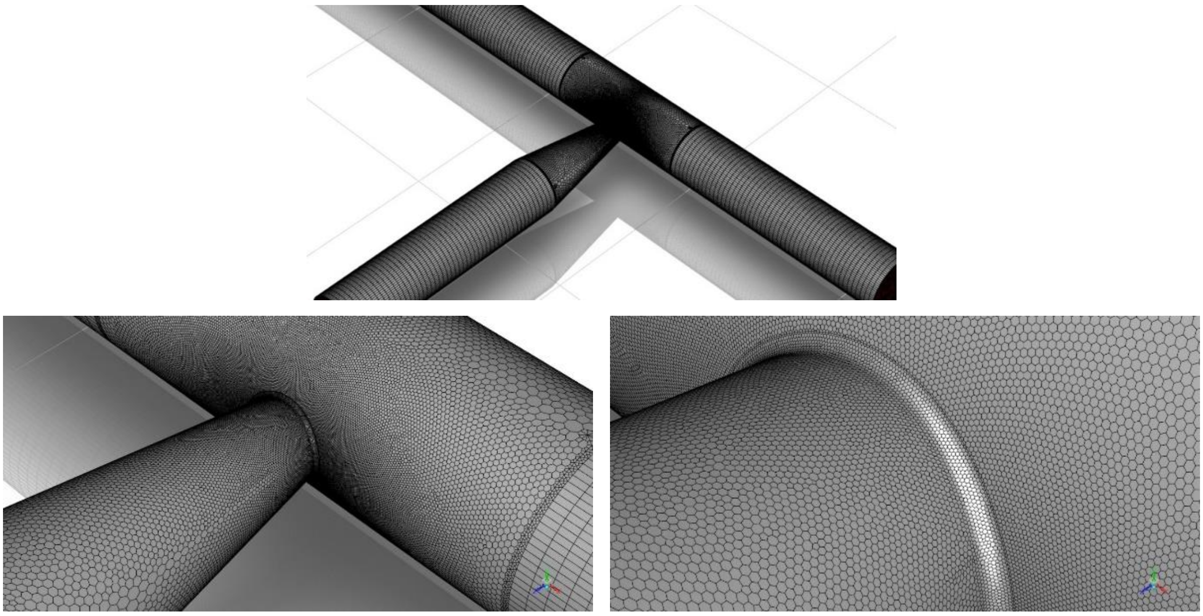

Figure 3. Meshing.

3. RESULTS AND DISCUSSION

Figure 4 shows velocity and turbulence kinetic energy for C_D of 0.7 with 10 m/s bulk velocity, from CFD simulation result. From the velocity field, it is known that velocity at branch pipe is around 1 – 2 m/s, while velocity at the main pipe is around 11 m/s. The turbulence kinetic energy reach is 1.32 m^2/s^2, while in the main pipe is near zero. These phenomena indicate thathigh turbulence occurs around the neck of the venturi.

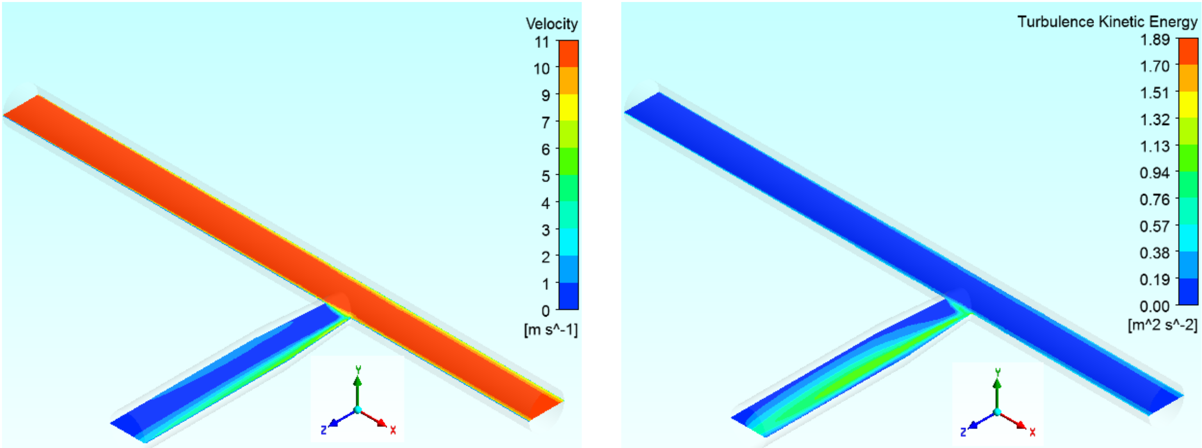

Figure 4. Velocity and turbulence kinetic energy for C_D of 0.7 with 10 m/s bulk velocity.

Figure 5 shows flow coefficient C_f (branch outlet to inlet debit ratio, Q_3/Q_1) against inlet velocity and Reynolds number (Re_D) for various diameter coefficient C_D (d/D). The figure shows that, the higher the diameter coefficient, the higher the flow coefficient. And the higher Reynolds number (Re_D), the higher the flow coefficient. And the higher velocity at the inlet pipe, the higher the flow coefficient. The effect of the Reynolds number tends to diminish at high Reynolds numbers.

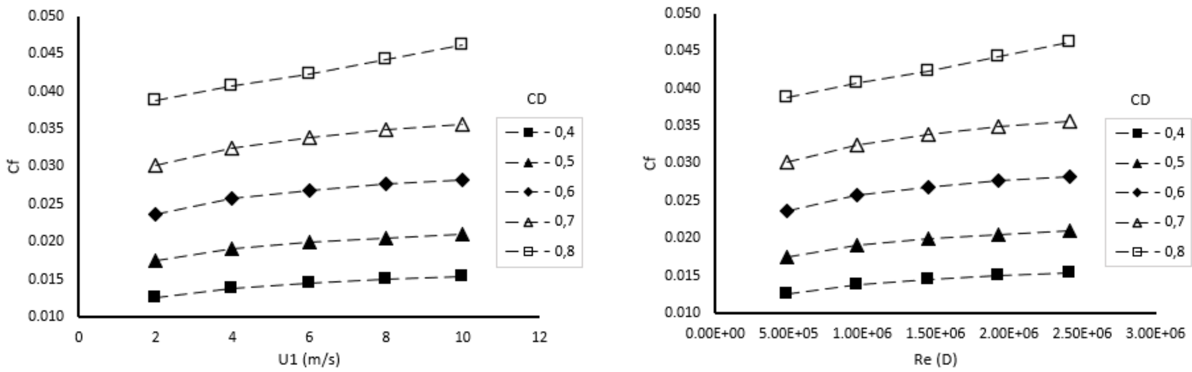

Figure 5. Flow coefficient against velocity and Re_D.

From Figure 5, it is known, that C_f is a function of Re_D and C_D. For convenience, the flow coefficient, C_f will be presented in the form of a non-dimensional variable group equation, as shown by Equation (1), as suggested by dimensional analysis.

$$C_f = aRe_D^b C_D^c \tag{1}$$

Natural logarithmic is applied to both sides of the equation. Equation (1) then turns to Equation (2).

$$\ln C_f = \ln a + b \ln Re_D + \ln C_D \tag{2}$$

To find a, b, and c, multiple regression from commercial Microsoft Excel was used. With a confidence level of 95%, the result of the last step is presented in Table 1, the regression statistic presented in Table 2.

Table 1. Obtained parameters.

Parameters	Coefficients	Standard Error
Intercept (ln a)	-4.427	0.102
ln Re_D	0.111	0.007
ln C_D	1.589	0.017

Table 2. Regression statistics.

Parameters	Value
Multiple R	0.999
R square	0.998
Adjusted R square	0.997
Standard error	0.021
Observations	25

Therefore, Equation (1) turn to:

$$C_f = 0.01195\, Re_D^{0.111} C_D^{1.589} \quad (3)$$

Comparing the original CFD simulation result with Cf value obtained from Equation (3), the maximum residual was 0.00159. It is 3.35% of the CFD simulation result.

4. CONCLUSION

From the simulation results, an equation correlation of dimensionless group of variables was constructed using multiple regression. The equation is shown by Equation (3). The maximum difference between the flow coefficient obtained from the curve fitting equation and the CFD simulation results is 3.35%.

REFERENCES

[1] Armah, E. K., Chetty, M., Adedeji, J. A., Kukwa, D. T., Mutsvene, B., Shabangu, K. P., & Bakare, B. F. (2021). Emerging trends in wastewater treatment technologies: the current perspective. *Promis Tech Wastewater Treat Water Qual Assess*, **1**, 71.

[2] Wijakmatee, T., Hemra, N., Wongsakulphasatch, S., Narataruksa, P., Cheenkachorn, K., & Prapainainar, C. (2021). Process intensification of biodiesel production with integrated microscale reactor and separator. *Chemical Engineering and Processing-Process Intensification*, **164**, 108422.

[3] Cruz-Díaz, M. R., Laureano, A., Rodríguez, F. A., Arenas, L. F., Pijpers, J. J., & Rivero, E. P. (2021). Modelling of flow distribution within spacer-filled channels fed by dividing manifolds as found in stacks for membrane-based technologies. *Chemical Engineering Journal*, **423**, 130232.

[4] Zhang, H., Kopfmüller, T., Achermann, R., Zhang, J., Teixeira, A., Shen, Y., & Jensen, K. F. (2020). Accessing multidimensional mixing via 3D printing and showerhead micromixer design. *AIChE Journal*, **66**(4), e16873.

[5] Fu, W. C., MacQueen, P. M., & Jamison, T. F. (2021). Continuous flow strategies for using fluorinated greenhouse gases in fluoroalkylations. *Chemical Society Reviews*, **50**(13), 7378–7394.

[6] Siddiqui, O. K., & Zubair, S. M. (2017). Efficient energy utilization through proper design of microchannel heat exchanger manifolds: A comprehensive review. *Renewable and Sustainable Energy Reviews*, **74**, 969–1002.

[7] Zhou, J., Sun, Z., Ding, M., Bian, H., Zhang, N., & Meng, Z. (2017). CFD simulation for flow distribution in manifolds of central-type compact parallel flow heat exchangers. *Applied Thermal Engineering*, **126**, 670–677.

[8] Duan, C., Liu, Z., Zhu, C., Ma, Y., & Fu, T. (2020). Distribution of gas-liquid two-phase flow in parallel microchannels with the splitting of the liquid feed. *Chemical Engineering Journal*, **398**, 125630.

[9] Kartaev, E. V., Emelkin, V. A., Ktalkherman, M. G., Aulchenko, S. M., & Vashenko, S. P. (2018). Upstream penetration behavior of the developed counter flow jet resulting from multiple jet impingement in the crossflow of cylindrical duct. *International Journal of Heat and Mass Transfer*, **116**, 1163–1178.

[10] Xie, F., Li, Y., Wang, X., Chen, E., Wang, L., & Xia, S. (2019). Experimental investigation of abnormal pressure drop in branch feedlines with a five-port spherical cavity in liquid oxygen engines. *Cryogenics*, **104**, 102994.

[11] Hassan, J. M., Mohamed, T. A., Mohammed, W. S., & Alawee, W. H. (2014). Modeling the uniformity of manifold with various configurations. *Journal of Fluids*, **2014**(1), 325259.

[12] Conte, G. & Azzopardi, B. J. (2003). Film thickness variation about a T-junction. *International Journal of Multiphase Flow*, **29**(2), 305–328.

[13] Wang, L. Y., Wu, Y. X., Zheng, Z. C., Guo, J., Zhang, J., & Tang, C. (2008). Oil-water two-phase flow inside T-junction. *Journal of Hydrodynamics*, **20**(2), 147–153.

[14] Azzopardi, B. J., Colman, D. A., & Nicholson, D. (2002). Plant application of a T-junction as a partial phase separator. *Chemical Engineering Research and Design*, **80**(1), 87–96.

[15] Sugianto, S., Puspitasari, D., Indarto, I., & Khasani, K. (2010, October). Simulasi numerik pemisahan aliran dua fase liquid-liquid di dalam T-junction. *Prosiding Industrial Research Workshop and National Seminar*, **1**, 2.

[16] Tran, M., Memon, Z., Saieed, A., Pao, W., & Hashim, F. (2018). Numerical simulation of two-phase separation in T-junction with experimental validation. *Journal of Mechanical Engineering and Sciences*, **12**(4), 4216–4230.

[17] Wu, H., Zhou, X., & Ma, J. (2019). Simulation of T-junctions two phases separation characteristics. *Vibroengineering Procedia*, **26**, 100–105.

[18] Yang, L., Wang, J., Ma, Y., & Zou, L. (2019). Phase split of oil-water two phase flow at double-layer T-junctions pipes. *IOP Conference Series: Earth and Environmental Science*, **384**(1), 012061.

[19] Berman, E. T., Setiawan, A., & Arifianto, E. S. (2018). Evaluation of performance an air conditioning systems using t-junction flash gas refrigerant. *IOP Conference Series: Materials Science and Engineering*, **288**(1), 012064.

[20] Li, X. & Wang, S. (2013). Flow field and pressure loss analysis of junction and its structure optimization of aircraft hydraulic pipe system. *Chinese Journal of Aeronautics*, **26**(4), 1080–1092.

[21] Azzopardi, B. T. & Whalley, P. B. (1982). The effect of flow patterns on two-phase flow in a T junction. *International Journal of Multiphase Flow*, **8**(5), 491–507.

[22] Azzopardi, B. J. & Smith, P. A. (1992). Two-phase flow split at T junctions: effect of side arm orientation and downstream geometry. *International Journal of Multiphase Flow*, **18**(6), 861–875.

[23] Wren, E. & Azzopardi, B. J. (2004). Affecting the phase split at a large diameter T-junction by using baffles. *Experimental thermal and fluid science*, **28**(8), 835–841.

[24] Yang, L. & Azzopardi, B. J. (2007). Phase split of liquid–liquid two-phase flow at a horizontal T-junction. *International Journal of Multiphase Flow*, **33**(2), 207–216.

[25] Penmatcha, V. R., Ashton, P. J., & Shoham, O. (1996). Two-phase stratified flow splitting at a T-jun. *International journal of multiphase flow*, **22**(6), 1105–1122.

[26] Rodriguez, O. M. H. & Oliemans, R. V. A. (2006). Experimental study on oil–water flow in horizontal and slightly inclined pipes. *International Journal of Multiphase Flow*, **32**(3), 323–343.

[27] Lu, G. Y., Wang, J., & Jia, Z. H. (2007). Experimental and numerical investigations on horizontal oil-gas flow. *Journal of Hydrodynamics*, **19**(6), 683–689.

[28] Margaris, D. P. (2007). T-junction separation modelling in gas–liquid two-phase flow. *Chemical Engineering and Processing: Process Intensification*, **46**(2), 150–158.
[29] Liow, J. (2004). Numerical simulation of drop formation in a T-shaped microchannel. *15th Australasian Fluid Mechanics Conference*.
[30] Bhramara, P., Rao, V. D., Sharma, K. V., & Reddy, T. K. K. (2009). CFD analysis of two phase flow in a horizontal pipe–prediction of pressure drop. *Momentum*, **10**, 476–482.
[31] Yang, L., & Zhang, C. L. (2005). Two-fluid model of refrigerant two-phase flow through short tube orifice. *International Journal of Refrigeration*, **28**(3), 419–427.
[32] Carlson, A., Kudinov, P., & Narayanan, C. (2008). Prediction of two-phase flow in small tubes: a systematic comparison of state-of-the-art CMFD codes. *5th European Thermal-Sciences Conference*, *The Netherlands*, 126–130.